Letter | Vol. 44, No. 18 / 15 September 2019 / Optics Letters 4455

Optics Letters

# Anti-scattering effect analyzed with an exact theory of light scattering from rough multilayers

G. Soriano,[1,*] M. Zerrad,[1] and C. Amra[1]

Aix-Marseille Université, CNRS, Centrale Marseille, Institut Fresnel, UMR 7249, 13013 Marseille, France
*Corresponding author: gabriel.soriano@fresnel.fr

Received 23 July 2019; revised 13 August 2019; accepted 14 August 2019; posted 14 August 2019 (Doc. ID 373073); published 6 September 2019

**First-order theories of light scattering previously revealed the existence of anti-scattering effects in optical multilayers. Here we present an exact electromagnetic theory that is able to complete the scattering analysis when first-order scattering is cancelled. The theory is valid for arbitrary rough multilayers.** 

https://doi.org/10.1364/OL.44.004455

Light scattering from slightly rough multilayers [1–5] has been extensively studied in the field of optical interference coatings [6,7]. Such planar multilayers most often consist of dielectric materials produced with vacuum deposition technologies (electron beam deposition, ion assisted deposition, dual ion beam sputtering, magnetron sputtering) which allow materials to grow in amorphous thin film form on fused silica substrates and others. It is well known [2,3,5] that in the optical bandpass of spatial frequencies [8], substrate roughness is replicated from one interface to another within these multilayers, and that this replication effect creates a roughness threshold which is most often responsible for the major scattering contribution. Since polishing techniques have allowed the reduction of substrate roughness to values down to a fraction of nanometer, all interfaces of optical coatings are slightly rough; this is the reason why first-order electromagnetic theories have shown great success when analyzing angular and wavelength scattering patterns from these components. Numerous results can be found [2,3,5] that emphasize an excellent agreement between theory and experiment, even for complex coatings involving hundreds of layers.

However, there are a few situations where the first-order theory must be completed, even though the surfaces are slightly rough. One iconic situation is that of the anti-scattering effect that was shown [9,10] to occur at specific angles or wavelengths, due to destructive interferences between waves scattered from different fully correlated surfaces. In this case, the first-order scattering is perfectly cancelled, while low-level signals can still be measured and must be taken into account; indeed, for an increasing number of applications (complex micro-filters for space multiplexing, mirrors for gravitational-wave detection), the energy balance (including reflection, transmission, absorption, and scattering) must be known with an absolute accuracy of 1 ppm (1 ppm $= 10^{-6}$). Hence, facing this difficulty requires a higher-order theory [11–13], or rather an exact electromagnetic theory [14,15], which is able to predict light scattering from arbitrary rough multilayers.

Though different formalisms [16–18] were developed to take account of arbitrary roughness at one single (uncoated) surface, until now, only a few of them have addressed the case of multilayers [19]. The goal of this Letter to present an exact electromagnetic theory based on an extension of the boundary integral equation (BIE) method [18,20–22]. A numerical calculation is given in two-dimensional scattering configuration [23] for single layers involving a set of roughness parameters [24], allowing the anti-scattering effect to occur, and the results are focused on a comparison with a first-order theory.

We consider a three homogeneous media problem (see Fig. 1) where the layer $\Omega_2$ is bounded by two non-intersecting rough surfaces $\Sigma_n$ with equations $z = z_n + h_n(\mathbf{r})$ for $n = 1, 2$ in the Cartesian coordinates $(x, y, z)$, and denoting $(x, y) = \mathbf{r}$. It is assumed that the two boundaries do not overlap; that is, $z_1 + h_1(\mathbf{r}) > z_2 + h_2(\mathbf{r})$ for all $\mathbf{r}$. The layer is enlightened from superstrate $\Omega_1 : z > z_1 + h_1(\mathbf{r})$ through interface $\Sigma_1$. A wavelength in vacuum is denoted $\lambda_0$, so that angular frequency is $\omega = 2\pi c/\lambda_0$. Surface $\Sigma_2$ interfaces the layer from substrate $\Omega_3$. Electromagnetic parameters at wavelength $\lambda_0$ are denoted $(\varepsilon_m, \mu_m)$ with $m = 1$ in the superstrate, $m = 2$ in the layer and $m = 3$ in the substrate.

Assuming an $e^{-i\omega t}$ implicit time-dependency, the electromagnetic field $(\mathbf{E}, \mathbf{H})$ satisfies in domain $\Omega_m$ the time-harmonic Maxwell's equations $\mathbf{curl}\mathbf{E} = +i\omega\mu_m\mathbf{H}$ and $\mathbf{curl}\mathbf{H} = -i\omega\varepsilon_m\mathbf{E}$. The tangential components of the field $\hat{\mathbf{n}}_p \times \mathbf{E}$ and $\hat{\mathbf{n}}_p \times \mathbf{H}$ on both interfaces $p = 1, 2$ are continuous. $\hat{\mathbf{n}}_p$ denotes the unit normal vector, oriented from $\Omega_{p+1}$ toward $\Omega_p$. This field also satisfies an outgoing wave condition in the substrate $\Omega_3$. The incident field $(\mathbf{E}^{\mathrm{inc}}, \mathbf{H}^{\mathrm{inc}})$ satisfies the Maxwell's equations for $m = 1$, but in the whole space. It writes as a sum of downward-directed plane waves:

$$\mathbf{E}^{\mathrm{inc}}(\mathbf{r}, z) = \int_{\mathrm{IR}^2} \mathbf{E}_1^{0-}(\mathbf{k}) e^{i(\mathbf{k}\cdot\mathbf{r} - q_1 z)} \mathrm{d}\mathbf{k}, \tag{1}$$

with $\mathbf{k}^2 + q_1^2 = \omega^2\varepsilon_1\mu_1$ and $0 \le \arg q_1 \le \pi/2$. The scattered field $(\mathbf{E} - \mathbf{E}^{\mathrm{inc}}, \mathbf{H} - \mathbf{H}^{\mathrm{inc}})$ satisfies an outgoing wave condition in the superstrate.

0146-9592/19/184455-04 Journal 

The reference field $(\mathbf{E}^0, \mathbf{H}^0)$ corresponds to the field $(\mathbf{E}, \mathbf{H})$ in the case where the layer surfaces are two parallel planes $z = z_1$ and $z = z_2$. The plane wave decompositions of the reference field in the three media write

$$\int_{\mathrm{IR}^2} \{\mathbf{E}_m^{0+}(\mathbf{k}) e^{i(\mathbf{k}\cdot\mathbf{r}+q_m z)} + \mathbf{E}_m^{0-}(\mathbf{k}) e^{i(\mathbf{k}\cdot\mathbf{r}-q_m z)}\} \mathrm{d}\mathbf{k} = \mathbf{E}_m^0(\mathbf{r}, z), \tag{2}$$

with $\mathbf{k}^2 + q_m^2 = \omega^2 \varepsilon_m \mu_m$ and $0 \leq \arg q_m \leq \pi/2$. Outgoing wave condition in the substrate leads to $E_3^{0+}(\mathbf{k}) = \mathbf{0}$ for all $\mathbf{k}$. In Eq. (2), those three plane wave decompositions are extended to the whole space to define the three fields $(\mathbf{E}_m^0, \mathbf{H}_m^0)$.

Now, for rough interfaces, the tangential components of the field $\hat{\mathbf{n}}_p \times \mathbf{E}$ and $\hat{\mathbf{n}}_p \times \mathbf{H}$, cast into the vector form

$$X = \begin{bmatrix} \hat{\mathbf{n}}_1 \times \mathbf{E} \\ \hat{\mathbf{n}}_1 \times \mathbf{H} \\ \hat{\mathbf{n}}_2 \times \mathbf{E} \\ \hat{\mathbf{n}}_2 \times \mathbf{H} \end{bmatrix}, \tag{3}$$

satisfy the linear system

$$A(X - Y) = C(Z - Y), \tag{4}$$

of coupled BIEs. The two vectors

$$Y = \begin{bmatrix} \hat{\mathbf{n}}_1 \times \mathbf{E}_1^0 \\ \hat{\mathbf{n}}_1 \times \mathbf{H}_1^0 \\ \hat{\mathbf{n}}_2 \times \mathbf{E}_2^0 \\ \hat{\mathbf{n}}_2 \times \mathbf{H}_2^0 \end{bmatrix} \quad Z = \begin{bmatrix} \hat{\mathbf{n}}_1 \times \mathbf{E}_2^0 \\ \hat{\mathbf{n}}_1 \times \mathbf{H}_2^0 \\ \hat{\mathbf{n}}_2 \times \mathbf{E}_3^0 \\ \hat{\mathbf{n}}_2 \times \mathbf{H}_3^0 \end{bmatrix}, \tag{5}$$

are determined from the reference field on the rough boundaries. Matrix $A$ writes

$$A = \begin{bmatrix} \frac{1}{2} - \mathcal{K}_1^{11} & -\mu_1 \mathcal{T}_1^{11} & 0 & 0 \\ \frac{1}{2} + \mathcal{K}_2^{11} & +\mu_2 \mathcal{T}_2^{11} & -\mathcal{K}_2^{12} & -\mu_2 \mathcal{T}_2^{12} \\ +\mathcal{K}_2^{21} & +\mu_2 \mathcal{T}_2^{21} & \frac{1}{2} - \mathcal{K}_2^{22} & -\mu_2 \mathcal{T}_2^{22} \\ 0 & 0 & \frac{1}{2} + \mathcal{K}_3^{22} & +\mu_3 \mathcal{T}_3^{22} \end{bmatrix}, \tag{6}$$

introducing (notations are derived from [25] and generalized to layered media) the electric field integral equation (EFIE) operator

$$\mathcal{T}_m^{np} \mathbf{j}(\mathbf{R}_n) = \hat{\mathbf{n}}_n \times \int_{\Sigma_p} i\omega \bar{\mathbf{G}}_m(\mathbf{R}_n - \mathbf{R}_p) \cdot \mathbf{j}(\mathbf{R}_p) \mathrm{d}S_p, \tag{7}$$

and the magnetic field integral equation (MFIE) operator

$$\mathcal{K}_m^{np} \mathbf{j}(\mathbf{R}_n) = \hat{\mathbf{n}}_n \times \int_{\Sigma_p} \mathbf{curl} \bar{\mathbf{G}}_m(\mathbf{R}_n - \mathbf{R}_p) \cdot \mathbf{j}(\mathbf{R}_p) \mathrm{d}S_p, \tag{8}$$

with $\mathbf{j}$ a tangential vector field and for two points $\mathbf{R}_n$ and $\mathbf{R}_p$ on interfaces $\Sigma_n$ and $\Sigma_p$, respectively. Those operators involve the free-space dyadic Green's functions $\bar{\mathbf{G}}_m(\mathbf{R}) = (\bar{\mathbf{I}} + K_m^{-2} \mathbf{grad}\, \mathrm{div}) G_m(\mathbf{R})$. For passive media $m = 1, 2, 3$, the wavenumbers $K_m$ satisfy $K_m^2 = (2\pi/\lambda)^2 \varepsilon_m \mu_m$ with $0 \leq \arg K_m \leq \pi/2$. The scalar Green's functions are driven by equations $(\mathrm{div}\, \mathbf{grad} - K_m^2) G_m(\mathbf{R}) = -\delta(\mathbf{R})$ and radiation condition. Matrix $C$,

$$C = \begin{bmatrix} 0 & 0 & 0 & 0 \\ \frac{1}{2} + \mathcal{K}_2^{11} & +\mu_2 \mathcal{T}_2^{11} & 0 & 0 \\ +\mathcal{K}_2^{21} & +\mu_2 \mathcal{T}_2^{21} & 0 & 0 \\ 0 & 0 & \frac{1}{2} + \mathcal{K}_3^{22} & +\mu_3 \mathcal{T}_3^{22} \end{bmatrix}, \tag{9}$$

is a sparsified version of matrix $A$. Such a theory can easily be extended to structures with an arbitrary number of layers.

Then the scattered electric field writes in the $z > z_1 + \max h_1$ region of the superstrate as the sum of plane waves:

$$(\mathbf{E} - \mathbf{E}^{\mathrm{inc}})(\mathbf{r}, z) = \int_{\mathrm{IR}^2} \mathbf{E}^+(\mathbf{k}) e^{i(\mathbf{k}\cdot\mathbf{r}+q_1 z)} \mathrm{d}\mathbf{k}. \tag{10}$$

Their amplitude is related to the tangential components of the fields on $\Sigma_1$ through the expression

$$\mathbf{E}^+(\mathbf{k}) = +\frac{\mathbf{K}_1}{8\pi^2 q_1} \times \int_{\Sigma_1} \left\{ \frac{\mathbf{K}_1}{\omega \varepsilon_1} \times (\hat{\mathbf{n}}_1 \times \mathbf{H}) - \hat{\mathbf{n}}_1 \times \mathbf{E} \right\} e^{-i\mathbf{K}_1 \cdot \mathbf{R}_1} \mathrm{d}S_1, \tag{11}$$

with $\mathbf{K}_1 = \mathbf{k} + q_1 \hat{\mathbf{z}}$ being the upward-directed wavevector.

Finally, this electric field formulation is turned into a magnetic field formulation by substituting $\mathbf{E} \leftrightarrow \mathbf{H}$ and $\mu \leftrightarrow -\varepsilon$ in Eqs. (1)–(6) and Eqs. (9)–(11).

Because a numerical calculation is highly time consuming, the BIE theory (4) was implemented for one-dimensional surfaces and discretized with the method of moments [23]. A first step consisted of a direct comparison with a first-order theory small perturbation method (SPM). For that, we considered a sample which is a non-absorbing high-index quarter-wave layer ($n_H e_H = \lambda_0/4$) at the illumination wavelength $\lambda_0 = 632.8$ nm, with $n_H = 2.3$ being the optical index and $e_H$ being the layer thickness. The superstrate is air ($n_1 = 1$), and the substrate is glass ($n_3 = 1.52$). The incident field is a Gaussian beam, centered on normal incidence ($i = 0°$) and with 1.5° divergence (tapering parameter [18] is $g = 8$ μm). Both surfaces have a Gaussian roughness with autocorrelation length $L = 300$ nm, and their cross-correlation coefficient [13] is denoted $\alpha$. In Fig. 2, their height root mean squares ($\delta_1 = \delta_2 = 5$ nm) are set identical, but the surface profiles can be fully cross-correlated ($\alpha = 1$) or totally cross-uncorrelated ($\alpha = 0$).

We observe in Fig. 2, where polarization is TM, a very high agreement with the first-order theory, due to the low roughness-to-wavelength ratio. Such agreement holds in the whole angular range and for the two extreme cases of cross-correlation. As a reminder, the cross-correlated ($\alpha = 1$) scattering takes account of interferences between the waves scattered by the

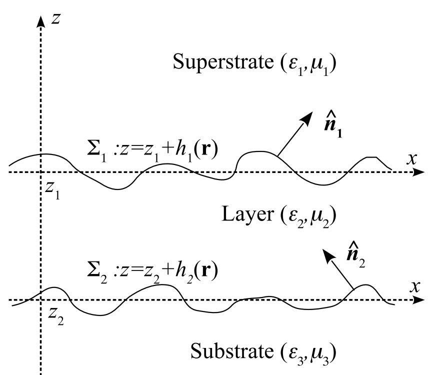


**Fig. 1.** Geometry of the problem.

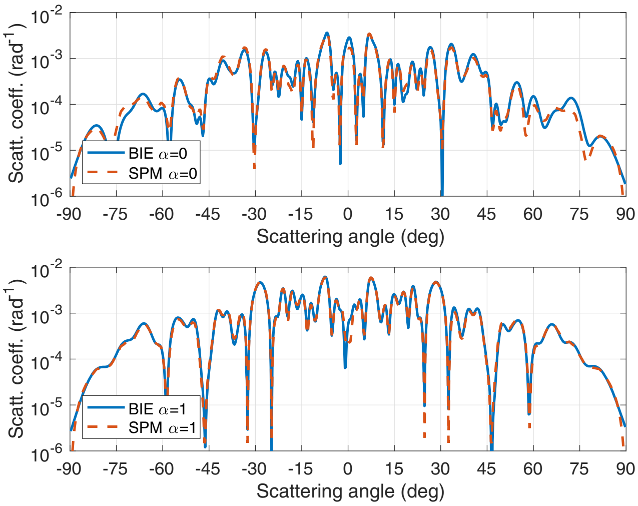


**Fig. 2.** Scattering diagram for a high-index quarter-wave layer at a 632.8 nm wavelength, normal incidence, and polarization TM. The roughness is 5 nm for both interfaces. The surface profiles are either totally uncorrelated ($\alpha = 0$, top plot) or fully correlated ($\alpha = 1$, bottom plot).

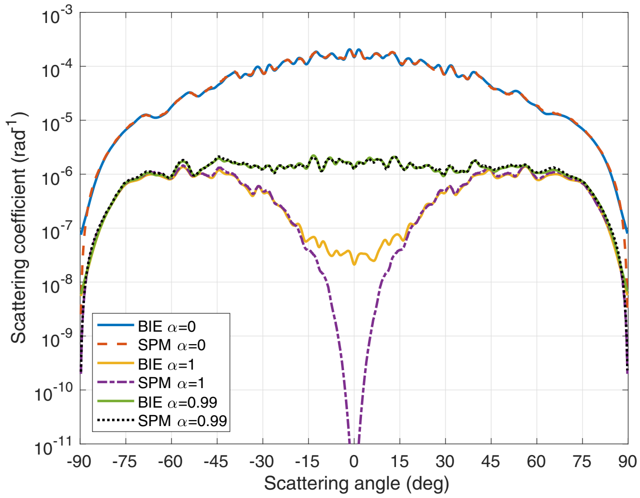


**Fig. 3.** Scattering diagram for a low-index quarter-wave layer at a 632.8 nm wavelength, normal incidence, and polarization TE. The layer-glass interface roughness is 5 nm, while the air-layer interface roughness satisfies the antiscattering condition (12).

two interfaces, while no interference occurs in the uncorrelated case ($\alpha = 0$). This is due to the fact that cross-correlation acts as a mutual coherence factor [9,10]. Hence, these first results validate the comparison with a first-order theory.

Now we focus the analysis on the anti-scattering effect [9] predicted with a first-order theory. Actually, in Ref. [9] it was shown that single layers may reveal an analytical zero of light scattering under the assumption of fully cross-correlated surfaces and specific roughness values. This effect is the result of destructive interferences between the waves scattered from surfaces $\Sigma_1$ and $\Sigma_2$, for which reason full cross-correlation is required. Furthermore, for these interferences to be destructive, the thin film should be low-index quarter-wave or high-index half-wave at the illumination wavelength $\lambda_0$. Eventually, the roughness ratio $\delta_1/\delta_2$ of the two surfaces must satisfy a condition related to the three index materials; that is [9],

$$\frac{\delta_1}{\delta_2} = \frac{n_2^2}{n_3^2}\frac{n_3^2 - n_2^2}{n_2^2 - n_1^2}, \tag{12}$$

for the low-index quarter-wave layer, and

$$\frac{\delta_1}{\delta_2} = \frac{n_2^2 - n_3^2}{n_2^2 - n_1^2}, \tag{13}$$

for the high-index half-wave layer. This last condition is given for a scattering cancellation at the scattering angle $\theta = 0°$.

In Figs. 3 and 4, we considered similar samples (single layers) and used our exact theory for a Monte Carlo comparison to a first-order theory under normal illumination. The Monte Carlo average is performed over 32 samples. The thin film materials are non-absorbing, and their real indices are given at the illumination wavelength $\lambda_0 = 632.8$ nm by $n_H = 2.3$ and $n_L = 1.3$. Such indices were given in Ref. [9] for ZnS and $Na_3AlF_6$ thin film materials. Hence, the optical thicknesses follow $n_H e_H = \lambda_0/2$ and $n_L e_L = \lambda_0/4$ with $e$ being the thickness. As previously, the (glass) substrate roughness is $\delta_1 = 5$ nm.

Figures 3 and 4, respectively, are given for the low-index quarter-wave layer in TE polarization and the high-index half-wave layer in TM polarization, with the roughness ratios given by Eqs. (12) and (13). As in Fig. 2, for the scattering from cross-uncorrelated rough profiles ($\alpha = 0$ curves on Figs. 3 and 4), we observe a high agreement between a first-order theory and the exact calculation in the whole angular range. As for the cross-correlated ($\alpha = 1$ curves on Figs. 3 and 4) scattering, the agreement still remains high for most scattering angles, but it fails in the close vicinity of the specular beam ($\theta = 0°$). Such a difference was expected, since first-order scattering is zero in this vicinity; hence, the remaining signal is characteristic of higher-order scattering. This result emphasizes the interest of an exact theory for further analysis of the anti-scattering effect.

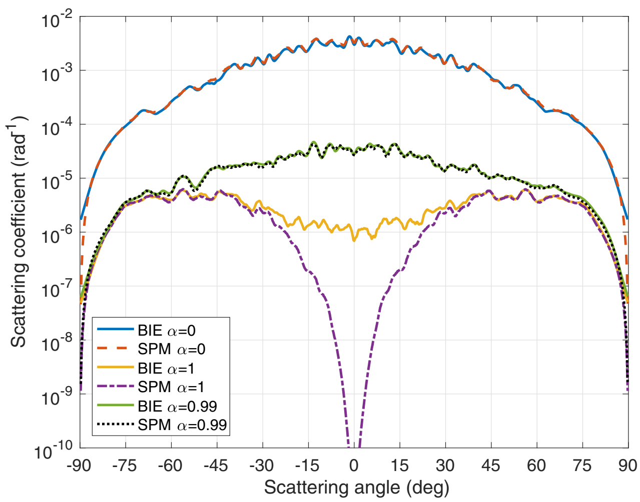


**Fig. 4.** Scattering diagram for a high-index half-wave layer at a 632.8 nm wavelength, normal incidence, and polarization TM. The layer-glass interface roughness is 5 nm, while the air-layer interface roughness satisfies the antiscattering condition (13).

However, before conclusion, it should be stressed that the analytical zero of first-order light scattering is highly sensitive to the cross-correlation coefficient around unity. Actually, even a slight departure from the value $\alpha = 1$ will break the interferential balance and increase the first-order signal. This is emphasized in Figs. 3 and 4, where first-order and exact scattering are also plotted for a cross-correlation value of $\alpha = 0.99$. With these supplementary curves, it is clear that the first-order scattering is far from zero at $\theta = 0°$, even though the variation in cross-correlation is only 1%. Furthermore, we observe that the two theories (first-order and exact) again reveal a high agreement for $\alpha = 0.99$, due to the fact that first-order scattering is again predominant. This result justifies why first-order calculation in multilayers is most often considered with cross-correlation values around 0.99 [5] (rather than 1), even more than a quasi-perfect (rather than perfect) replication of topography.

We have developed an exact electromagnetic theory of light scattering from arbitrary rough surfaces. The theory is a discretized set of coupled BIEs. However, with a modified right-hand side, it differs from the classical formulation [22]. Our approach was compared with great success to the first-order theory in the whole angular range. In order to emphasize higher-order scattering, we analyzed anti-scattering effects predicted by the first-order theory. The exact theory was able to quantify the scattering level when first-order scattering is zero. This is a key point, since new trends in optical coatings are about to take profit of the anti-scattering effect to minimize losses [26,27]. The exact theory might also lead, through future works, to the definition of improved anti-scattering conditions. We also quantified the sensitivity of scattering to interfaces cross-correlation. This allows us to establish a more accurate energy balance, as required in high-precision optical systems (pixelated filters for space micro-multiplexing, mirrors for detection of gravitational waves…). To conclude, this exact theory will also meet other applications in the field of radar probing of soil and moisture, cosmetics and living tissues, lighting, textiles, and stationery.

## REFERENCES


1. J. Elson, J. Rahn, and J. Bennett, Appl. Opt. **22**, 3207 (1983).
2. C. Amra, J. Opt. Soc. Am. A **11**, 197 (1994).
3. C. Amra, J. Opt. Soc. Am. A **11**, 211 (1994).
4. S. Schröder, T. Herffurth, H. Blaschke, and A. Duparré, Appl. Opt. **50**, C164 (2011).
5. M. Zerrad, S. Liukaityte, M. Lequime, and C. Amra, Appl. Opt. **55**, 9680 (2016).
6. H. A. Macleod and H. A. Macleod, *Thin-Film Optical Filters* (CRC Press, 2010).
7. P. W. Baumeister, Optimization **10**, 7 (2004).
8. C. Deumié, R. Richier, P. Dumas, and C. Amra, Appl. Opt. **35**, 5583 (1996).
9. C. Amra, G. Albrand, and P. Roche, Appl. Opt. **25**, 2695 (1986).
10. C. Amra, J. H. Apfel, and E. Pelletier, Appl. Opt. **31**, 3134 (1992).
11. M. Demir, J. Johnson, and T. Zajdel, IEEE Trans. Geosci. Remote Sens. **50**, 3374 (2012).
12. M. Sanamzadeh, L. Tsang, J. T. Johnson, R. J. Burkholder, and S. Tan, J. Opt. Soc. Am. A **34**, 395 (2017).
13. J.-P. Banon, Ø. S. Hetland, and I. Simonsen, Ann. Phys. **389**, 352 (2018).
14. C.-H. Kuo and M. Moghaddam, IEEE Trans. Antennas Propag. **54**, 2917 (2006).
15. M. Sanamzadeh, L. Tsang, and J. T. Johnson, IEEE Trans. Antennas Propag. **67**, 495 (2018).
16. C. Amra, C. Grèzes-Besset, and L. Bruel, Appl. Opt. **32**, 5492 (1993).
17. T. Elfouhaily and C. A. Guérin, Waves Random Media **14**, R1 (2004).
18. L. Tsang, J. A. Kong, K. H. Ding, and C. O. Ao, *Scattering of Electromagnetic Waves: Numerical Simulations*, Wiley Series in Remote Sensing (Wiley, 2001).
19. P. Imperatore, A. Iodice, M. Pastorino, and N. Pinel, Int. J. Antennas Propag. **2017**, Article ID 7513239 (2017).
20. D. Colton and R. Kress, *Integral Equation Methods in Scattering Theory* (SIAM, 2013), Vol. **72**.
21. W. Chew, M. Tong, and B. Hu, *Integral Equation Methods for Electromagnetic and Elastic Waves* (Morgan & Claypool, 2008).
22. N. Déchamps, N. de Beaucoudrey, C. Bourlier, and S. Toutain, J. Opt. Soc. Am. A **23**, 359 (2006).
23. C. Bourlier, N. Pinel, and G. Kubické, *Method of Moments for 2D Scattering Problems: Basic Concepts and Applications* (Wiley, 2013).
24. J. A. Ogilvy, *Theory of Wave Scattering from Random Rough Surfaces* (Adam Hilger, 1991).
25. G. Hsiao and R. Kleinman, IEEE Trans. Antennas Propag. **45**, 316 (1997).
26. J. Zhang, H. Wu, H. Jiao, S. Schröder, M. Trost, Z. Wang, and X. Cheng, Opt. Lett. **42**, 5046 (2017).
27. J. Zhang, H. Wu, I. V. Kozhevnikov, S. Shi, X. Cheng, and Z. Wang, Opt. Express **27**, 15262 (2019).